Residual Patterns of Alkyl Polyoxyethylene Surfactant Droplets after Water Evaporation

Scott M. Pierce,*,[†] Kwaichow B. Chan,[†] and Heping Zhu[‡]

Albany State University Department of Natural Sciences, 504 College Drive, Albany Georgia 31705
and United States Department of Agriculture, Agricultural Research Service, Application Research and
Technology Unit, Wooster, Ohio.

Using a nonionic, alkyl polyoxyethylene surfactant (X-77) in aqueous solutions, sessile droplet spreading, pinning, evaporation, contraction, and post-evaporation deposits are characterized. X-77 is widely used in the agricultural field as a spreader/adherent, intended to optimize pathenogenic agent coverage. Using a single droplet size under monitored temperature conditions, we control humidity, substrate hydrophobicity, and surfactant concentration to mimic varying agricultural conditions. For hydrophilic surfaces, the droplet spreads, reaching and retaining a maximum, stationary size. At this stage, a ring accretion occurs at the maximum spread diameter. During the final stage, the water film retracts, resulting in deposition of small islands of surfactant residue inside the ring. At lower concentrations of surfactant, we discover ring formations that break-up into "ring islands" at late-stage evaporation, accompanied by a distribution of the smaller islands in the interior portion of the substrate contact area. These are promoted by higher relative humidity. At higher concentrations, only a solid ring of surfactant remains, post-evaporation. Increasing surfactant concentration tends to increase the mean of the interior island size and to broaden the overall island size distribution. On sufficiently hydrophobic surfaces, surfactant-laden droplets do not evidence pinning, ring formations, or post-evaporation interior islands. Interestingly, lower humidity increases spreading at higher surfactant concentrations. Such pattern formations of surfactant deposit are reported for the first time and are of significance in projecting how surfactants such as X-77 distribute pesticides or other chemicals on leaf surfaces.

KEYWORDS: Surfactant pattern formation; Spray additive; Microdroplet island; Ring formation; Droplet spreading; Sessile droplet evaporation

INTRODUCTION

The objective of this research was to determine spreading, evaporation characteristics, evaporation dynamics characterizations, and post-evaporation deposit formations of nonionic surfactant-added droplets with various concentrations on two artificial target surfaces. It is hoped that this study will serve as a guide for field researchers to extrapolate surfactant behaviors from these target surfaces to specific applications, as required. Results of this study may also be used for developing new techniques and strategies to elucidate surfactant behaviors and patterns for leaf-specific applications in the future.

Pest control efficiency is greatly influenced by plant fine surface structure and plant growing conditions. For the plants with thick, waxy, or hairy leaf surfaces, the addition of surfactants in spray solutions can minimize variations in spray performance and improve pesticide effectiveness. The nonionic

surfactants are widely used as spray solution additives in pest control. The alkyl polyoxyethylene surfactant X-77, a product of Ortho Chemical (Chevron Chemical Co., San Francisco, CA), is one of the most popular nonionic surfactants commercially available because of its effectiveness and low cost. The substance is added to aqueous solutions of pesticides, herbicides, and fungicides to promote adhesion to targets, to allow ease of application through industrial spray mechanisms, via surface tension reduction, and to engender droplet spreading to maximize surface contact area.

A water-only droplet has a small contact area on waxy leaf surfaces. However, a water droplet containing X-77 in a durable emulsion can easily spread on these surfaces, becoming a thin layer deposited over the greater portion of the leaf's area. This phenomenon brings about the questions: how long will the surfactant-laden droplet last, that is, what is the evaporation time of a sessile droplet? What is the exact morphology and deposit pattern of the surfactant, after evaporation, that may influence the deposition of pesticides or other chemicals?

Leaf fine surface structure varies greatly with species, varieties, and ages. There is no standard for defining the category

* Author to whom correspondence should be addressed. Phone: (229) 430-1654, fax: (229) 430-4765, e-mail: scottpierce.chem@gmail.com.
† Albany State University.
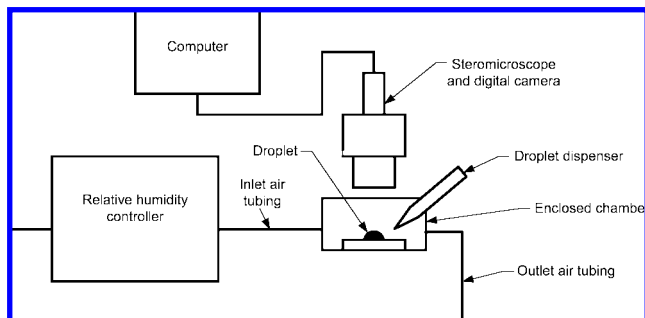‡ United States Department of Agriculture.

Figure 1. Schematic of the system setup to investigate the evaporation process of single droplets inside the environment-controlled chamber.

of leaf fine surfaces. In this study, the selection of two artificial surfaces, one hydrophilic and the other hydrophobic, covers a wide range of contact angles of sessile droplets and is intended to represent typical examples of leaf conditions. These surfaces allow much better contrast than leaves for imaging and provide controlled circumstances for comparisons.

Sessile droplet evaporation is a well-populated field of study (*1–4*). Dynamics within the droplet have also been chronicled (*5*). Here, previous work is enhanced to evaluate the deposition pattern of surfactant-laden droplets. As Deegan, Hu, and Larson revealed (*6–8*), a sessile droplet evaporates via a mechanism of internal flow wherein the liquid phase is abandoned preferentially at the triple phase line (pin line). For agricultural purposes, this is not desirable. Residues of chemicals would be deposited in a "coffee ring" at the droplet's pin line, reducing the available surface area covered to that of the ring. To what extent surfactant-laden water droplets suffer from the coffee-ring effect and how nonionic surfactants alter post-evaporation deposition patterns has not been fully characterized

and therefore deserves closer scrutiny in an agricultural context. Droplet evaporation using surfactants other than X-77 has been examined in previous work (*9–12*). There is no attempt made to duplicate this. Rather, we add to it in an attempt to enumerate the specific characteristics pertaining to this widely used product in a laboratory environment on the two selected surfaces.

Surfactant-induced pattern formation finds potential use in the biotech, nanoassembly, and agricultural fields (*13–17*). Here, the exemplar surfactant is used on two substrates, chosen to emphasize agricultural applications. The first is a simple soda lime glass microscope slide, a mildly hydrophilic substrate with an initial contact angle of ~40° with distilled water. Many field crops such as corn and soybeans have this approximate contact angle. The second is the same substance, but treated with a silane wax to represent a mildly hydrophobic substrate with an initial contact angle of ~90° with distilled water. Some floral crops such as poinsettia have contact angles of about 90°. A single droplet size (500 μm) is used, designed to be representative of a typical spray droplet. By capturing images of the droplet from above as it evaporates, we are able to plot substrate contact diameter against time to characterize spreading. By varying the surfactant concentration and external vapor phase conditions, the evaporation characteristics of these droplets over the most common agricultural range of use and humidity conditions (*18*) are examined. Finally, by analyzing chemical residues after water evaporation, the distribution of remaining surfactant, total contact surface area, and patterns formed are characterized. In so doing, an understanding of the most appropriate uses for agricultural purposes is achieved. In addition, spreading and distribution data herein presented may be of use in future work in the fields of self-assembly.
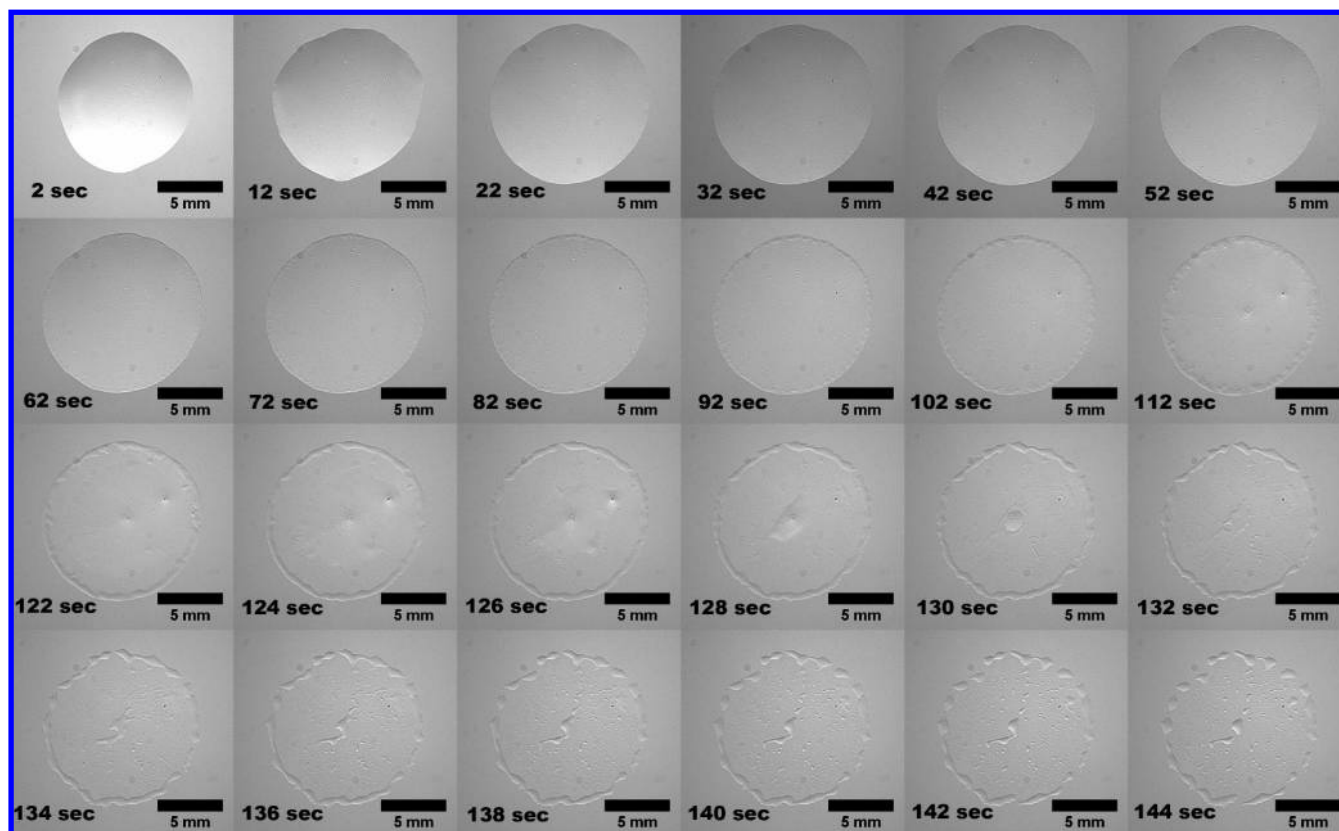

Figure 2. Time evolution of a 0.5% X-77 500 μm droplet on a mildly hydrophilic surface at 80% relative humidity.

Residual Patterns of Alkyl Polyoxyethylene Surfactant Droplets

J. Agric. Food Chem., Vol. 56, No. 1, 2008 **215**

Table 1. Summary of Results

| | droplet area | | | | | | | time (seconds) | |
	Max (mm^2)	Deposited (mm^2)	Spread (mm^2)	Post-evaporation area (mm^2)	% of max area covered final	% interior (nonring) coverage	Ave Island area (mm^2)	Spreading (seconds)	Evaporation (seconds)
Clean Glass Substrate									
0.5% x-77									
30% RH	78	54.5	23.5	22	28	31.5	0.06	17.5	73
80% RH	114	87	27	24.4	21	53.0	0.16	20	117
1% x-77									
30% RH	105	23	82	45.7	44	11.8	0.11	3.5	70
80% RH	76	52	24	67	88	9.9	0.07	6	83
						single islands post-evaporation:			
Rain-X Coated Glass Substrate									
0.5% x-77									
30% RH	65.5	51	14.5	2.8	4	100	2.8	4.2	112
80% RH	78.8	70	8.8	3.6	5	100	3.6	5.5	152
1% x-77									
30% RH	38.5	34.5	4	2.4	6	100	2.4	4.6	85
80% RH	38	26.5	11.5	5	13	100	5	15	91

MATERALS AND METHODS

A small environmental chamber was constructed for the experiments. A 10 cm section of a 6 mm Plexiglas tube was cut and sealed at each end with similar, planar, material. The tube was bored through for six ports. The first port was fitted with a hose that introduced air, which was microprocessor-controlled for temperature, velocity, and humidity. The second port exhausted the air and returned it, through a filter, to the control system. The third port allowed access for the syringe, which deposited droplets, and the forth allowed sensors to pass into the chamber. On one end, which became the top, a 6 cm quartz optical flat was let into the material to provide a viewport. The other was used as the base. The remaining two ports were threaded to allow external *X* and *Y* control of the substrate. This apparatus was placed on the base of a standard stereomicroscope (Olympus SZX-12 with DF Plapo1xPF objective, Center Valley, PA). Light was provided by a 120 V halogen light source with two external flexible fiber optic arms. The assembly provided relative humidity stability of ±3.5% with an ambient temperature of 22 °C. **Figure 1** is a representation of the working setup.

Smooth glass microscope slides, used for the mildly hydrophilic surfaces, were sonically cleaned with acetone and then methanol, each for ten minutes. The slides were stored in clean methanol until used. Before each test, a clean slide was removed, placed in the chamber, and allowed to dry for 10 min under a gentle stream of dry, clean air. Droplets, calibrated

to correspond to 500 μm in the spherical state, were placed individually via a pressure-driven syringe (Barnant Co, Model 400–1901 pump, Nordson EFD Ultra 2400 dispensing station and EFD precision tips, East Providence, RI). Once deposited, the syringe was withdrawn from view, but remained inside the chamber. After each evaporation period, the slide was relocated within the chamber to expose an untouched area and was replaced after approximately every five droplets.

Hydrophobic surfaces consisted of glass microscope slides as above. After removing a slide from the methanol bath and allowing it to dry under a large dust cover at laboratory conditions for approximately 10 min, the slide was treated with Rain-X Glass treatment (SOPUS products, Houston TX) via application with a chem-wipe. The wipe was moistened with Rain-X, an isopropanol-based silane solution, and applied to the slide in several directions of motion. The treated slide was then placed in the chamber and allowed to dry for approximately five minutes before droplets were deposited.

Images were taken every 0.5−2 s, depending on substrate, via CCD camera (Spot Insight Model 18.2 Diagnostic Instruments, Sterling Heights, MI) beginning before the droplet was placed and ending after evaporation had concluded. These images were sampled, post collection and based on data requirements, every 2–10 s in the 100–200 s evaporation period. Each sampled image was processed using ImageProPlus' polygonal autotrace feature (ver 4.1, Media Cybernetics, Bethesda, MD). This contrast recognition algorithm allowed for a standard error of repeatability for this analysis of 0.003793 mm^2. Size
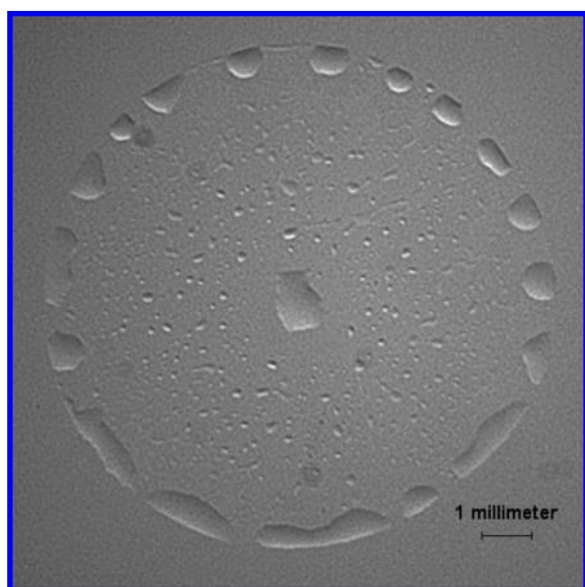

Figure 3. Final deposition pattern of 0.5% X-77 on a mildly hydrophilic substrate at 80% RH.
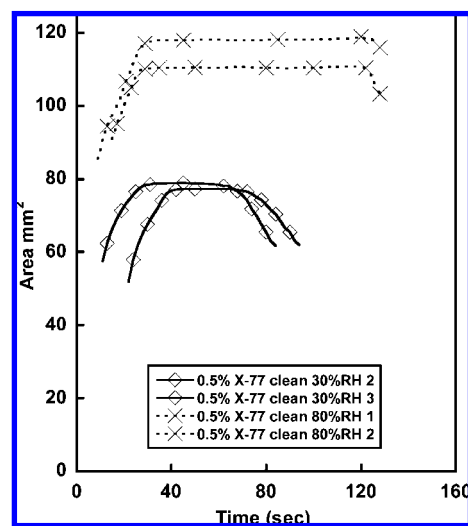

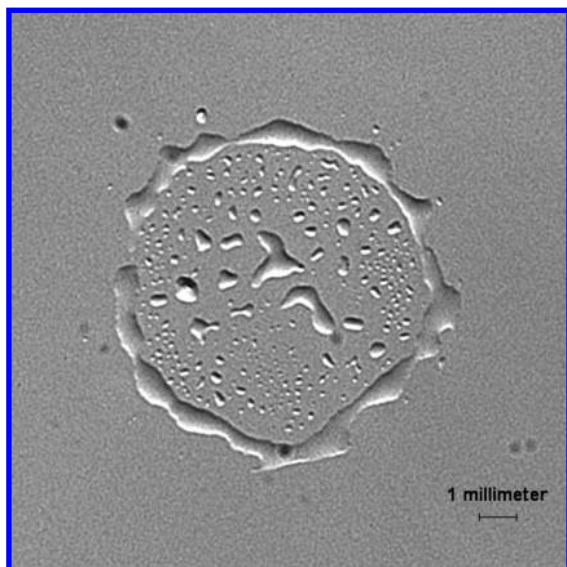**Figure 4.** Substrate contact diameter given 0.5% X-77 and 30 vs 80% RH.

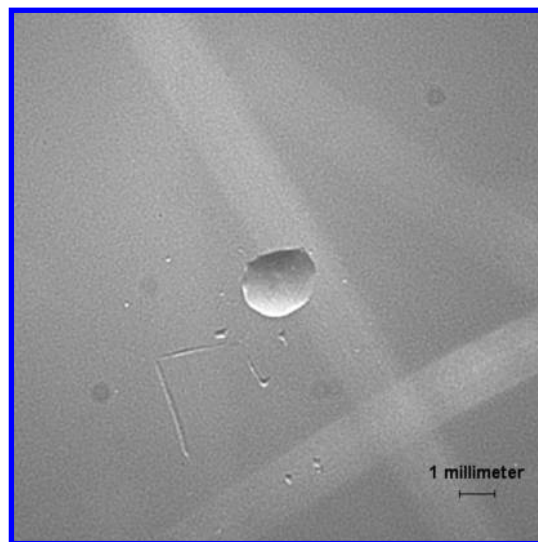**Figure 5.** Final deposition pattern of 0.5% X-77 on a mildly hydrophilic substrate at 30% RH.

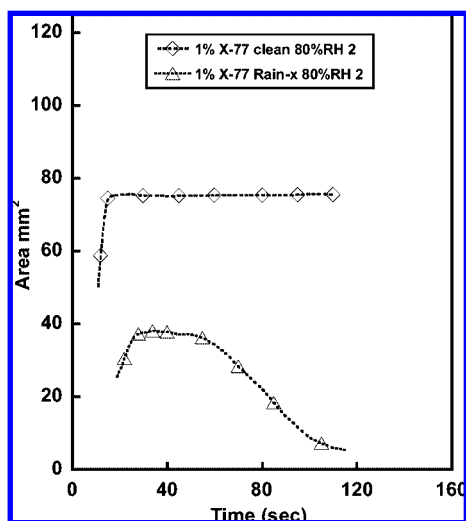**Figure 7.** Final deposition pattern of 0.5% X-77 on hydrophobic substrate at 80% RH.

Figure 6. Substrate area evolution; hydrophilic vs hydrophobic surfaces.

Figure 8. Higher concentration spreading at 30 and 80% RH.

calibrations were effected by capturing photographs at each focal length of a Zeiss 0.01 mm micrometer slide.

RESULTS AND DISCUSSION

General Evaporation Characterizations. The droplet spends the first twenty seconds spreading. After spreading ceases, sessile droplets on clean glass in high humidity conditions (80% RH) pin at the triple phase line through more than eighty percent of the evaporation period. Only at the very end of the period will the droplet shrink in diameter. **Figure 2** illustrates the time evolution of this process in 80% relative humidity. Also, see **Table 1** for a quick-reference summary of these results. Consistent with refs *5–8* above, it is thought that an internal flow is established in the evaporating droplet system such that fluid moves from the center, top portion of the droplet downward to the bottom of the droplet and then out, toward the triple phase line, wherein it leaves the liquid phase. As the water evaporates, the concentration of surfactant increases at the pin line until a ring begins to form by accretion at approximately 40% of the total period. As the evaporation progresses and as the contact angle approaches zero, the droplet reaches a point where it is
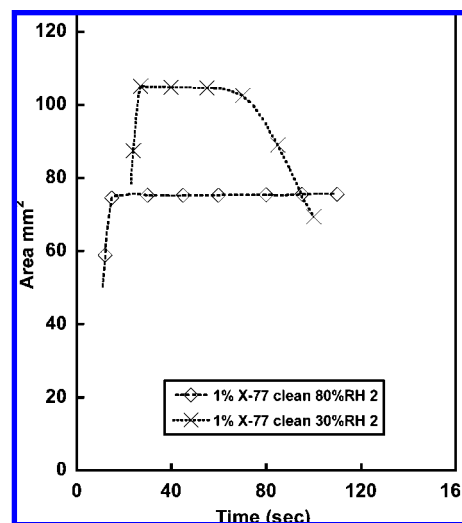
no longer able to maintain the supply of "fresh" (lower concentration) fluid to the flux area, and the droplet collapses. The surfactant-laden ring becomes variable in width and finally breaks apart, due to surface tension, forming "ring islands" close to the perimeter of the original contact area. These islands form (gather) only at the very end of the period. Meanwhile, in the interior of the droplet, the surfactant/water mixture is no longer able to flow outward to the pin line but remains in the center of the droplet deposition area. A single island is clearly visible at approximately 80% of the evaporation period. As the last of the water evaporates, the surfactant in the center of the droplet breaks apart in very small (as small as 100 nm) "islands", distributed throughout the interior portion of the droplet, usually with one larger island remaining in the center. The final pattern of 0.5% X-77 at 80% RH is illustrated in **Figure 3**. Thus, the X-77 addition is seen to have potential for increased phytotoxicity on plants via its ability to distribute active agents to a greater proportion of the droplet's original contact area, as opposed to simply depositing a ring at the triple phase line.

Lower relative humidity (lower partial fraction of evaporant in the surrounding vapor phase) encourages diffusion (evaporation). Thus, each phase of the process is truncated in time. Less spreading is observed, and thus the droplet's maximum diameter
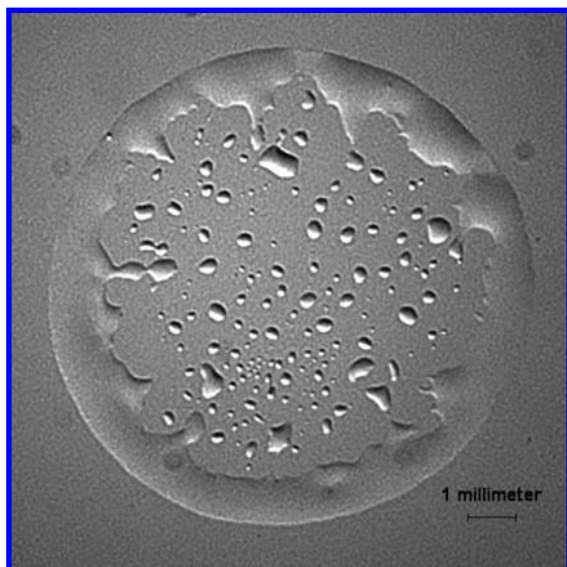
Figure 9. 1% X-77 post-evaporation pattern at 80% RH.

Figure 10. 1% X-77 post evaporation pattern formation at 30% RH.

is reduced. **Figure 4** plots the area evolution for 30% and 80% RH on glass substrates. Under low humidity conditions, droplet pin times are reduced from more than eighty percent of the post-spreading evaporation cycle to approximately fifty percent. Ring droplet and interior droplet island formations are more variable, suggesting internal convection patterns are not as regular as the drop evaporates. Interior island formations tend to be larger and fewer in number. Post-evaporation ring formations tend to be continuous, though variable in width. One observes this variability above but during the evaporation period. Here, truncated evaporation periods do not allow sufficient time for ring break-up. Thus, ring formations are restricted to a variable-width, continuous regime. **Figure 5** illustrates the final deposition pattern of 0.5% X-77 samples at 30% RH.

Hydrophobic surface characteristics reduce spreading, increase contact angle, and elongate evaporation time while decreasing droplet pinning time. In this case, droplet pinning does not persist through the majority of the evaporation period, and thus the outward flow to the pin line does not establish in the same way. **Figure 6** illustrates the area evolution of the hydrophobic substrate contrasted with that of clean glass. When the pin line retracts, outward convection is thought to decrease dramatically. As such, a ring does not form. Rather, the surfactant gathers in the center of the droplet's original contact area as a single (surfactant-only) droplet as evaporation proceeds. **Figure 7** illustrates the final deposition pattern of 0.5% X-77 on hydrophobic (Rain-X-coated) surface at 80% RH.

Droplet Evaporation Time. In all cases tested, droplets evaporate faster in lower humidity conditions and on hydrophilic substrates. In each case, higher concentrations of X-77 promoted overall evaporation rate. Presumably, this is due to water-soluble volatile components present in the product. It should be noted that this is more pronounced with higher humidity. That is, for the 500 μm droplet on the hydrophilic substrates at 80% RH, the average evaporation times are 117 s for the 0.5% concentration and 83 s for the 1% concentration. This is contrasted with the average evaporation times of 73 s for the 0.5% concentration and 70 s for the 1% concentration at 30% RH. Thus, desired evaporation times can be controlled more easily via surfactant concentration, given hydrophilic leaf surfaces, at higher relative humidities.

Surfactant Concentration Effects. One might anticipate successive surfactant additions, that is, higher concentration,
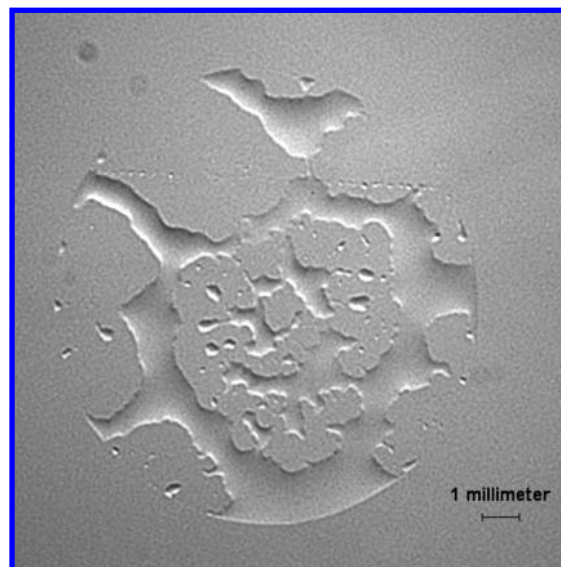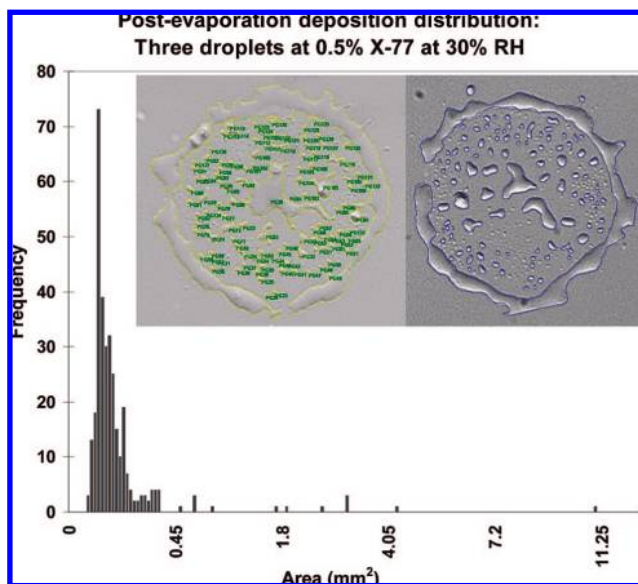

Figure 11. 0.5% X-77 post-evaporation deposition distribution for three droplets.

increasingly to promote spreading on hydrophilic surfaces, especially under higher-humidity conditions. This is the case for concentrations up to approximately 1%. Above this value, successive additions do not promote spreading under higher humidity conditions. In fact, the opposite is observed. Successive surfactant additions above 1% in high relative humidity conditions decrease droplet spreading. Above 1% concentration, more spreading is observed in *lower* humidity conditions (wherein evaporation occurs faster). See **Figure 8**, comparing area evolution of 1% surfactant concentration at 30% and 80% RH. This may be due to the complex balance between the lubricity of X-77 and water. Here, there is a critical point at which the one surpasses the other. At lower RH%, water evaporates faster while the surfactant remains behind. Below ~1% concentration, surfactant is not of sufficient concentration to dominate evaporation dynamics. Above that value, the surfactant dominates the dynamics of the internal droplet flow (with lower surface tension but with higher lubricity).

Given variable concentration, post-evaporation deposit patterns evidence similar humidity trends on hydrophilic surfaces. Given a
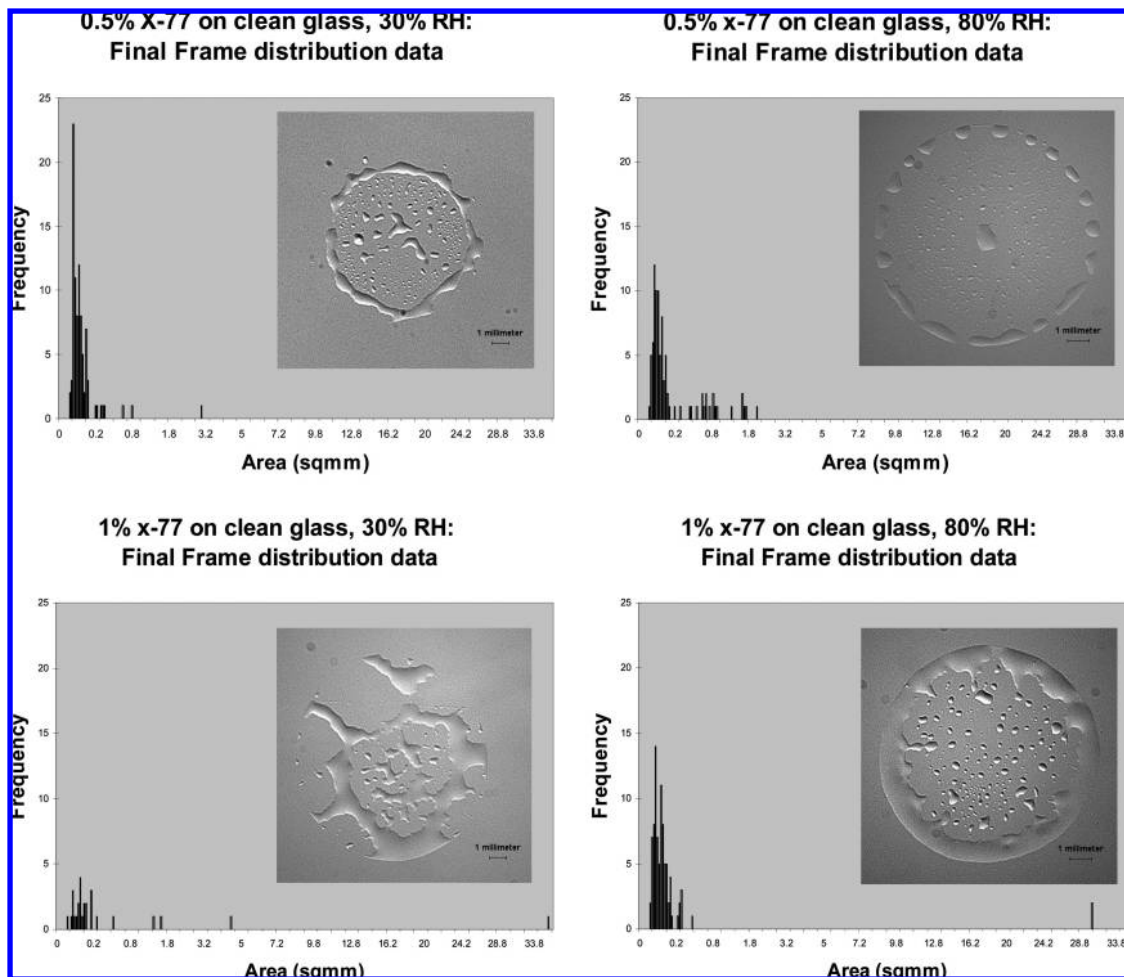
Figure 12. Final pattern and distribution comparisons of two concentrations at 30 and 80% RH.

1% concentration, higher humidity promotes pin-line ring and smaller interior droplet formations. Ring formations tend to be thicker with increasing concentration, whereas ring break-up into islands does not occur. Interior islands tend to be fewer and larger in size. See **Figure 9** for an illustration. Lower humidity truncates evaporation time, and thus does not allow the same flow characteristics to establish. Post-deposit formations are more variable and do not result in rings or ring islands. Rather, a discontinuous and unpredictable shape results. See **Figure 10** for an illustration. Hydrophobic substrate evaporations result in the same sort of single island formations. Increasing surfactant concentration simply increases the size of the final island formed.

The study also indicates that spray performance (droplet spreading) may be improved when pesticide spray mixtures containing surfactants at proper concentrations are applied under high relative humidity conditions. Droplet evaporation times are lengthened to approximately two minutes, thus affording enough of time for pesticides or chemicals to penetrate the leaf if so desired. If low humidity conditions prevail, maximum coverage can be achieved by properly increasing the surfactant concentration.

Post-evaporation Deposit Distributions. A combined distribution for three droplets at 0.5% X-77 and 30% RH is given in **Figure 11**, along with images of the data collection process. **Figure 12** is a summary of two concentrations at two RH% values, with their distributions, for comparison. Here, preliminary indications on hydrophilic surfaces are provided.

For a given concentration, increasing the relative humidity broadens the distribution. Disallowing the large ring formations in each reveals higher average interior island size with higher
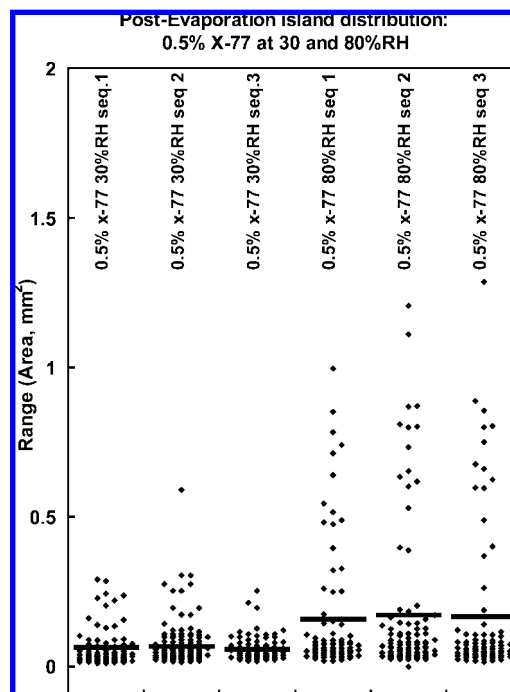

Figure 13. Post-evaporation interior island distributions.

humidity. **Figure 13** illustrates this with a dot-plot comparison of three droplets for each RH% at 0.5% surfactant concentration. Average values for 30% RH are on the order of 0.06 mm^2,

Residual Patterns of Alkyl Polyoxyethylene Surfactant Droplets

J. Agric. Food Chem., Vol. 56, No. 1, 2008 **219**

whereas those of the 80% RH are nearly three times as large, centering on 0.16 mm^2.

Total surface area covered by the surfactant post-evaporation is, as one might anticipate, largely a matter of the amount of surfactant present in the droplet. On hydrophilic substrates, a 0.5% concentration results in a total coverage of 24.43 mm^2 ± 3.56 (1σ) for 80% RH and 21.98 mm^2 ± 11.87 for 30% RH. This is approximately 20% and 28% of the maximum spread area of the droplet at 80% and 30% RH, respectively. Combining both relative humidities tested, the 1% concentration reveals a total coverage of 56.51 mm^2 ± 15.33. This total area coverage is roughly twice as large for the 1% droplet as that of the 0.5% droplet. However, the increased total coverage is not as well distributed over the target surface. Referring to **Table 1**, the percentage of post-evaporation surfactant nonring coverage (the percentage of surfactant remaining in the interior of the droplet) is markedly reduced by increased concentration. Although 53% of the surfactant's area consists of small islands in the 0.5% X-77 case at 80% RH, this percentage drops to just under 10% for the 1% X-77 case at the same humidity. Whereas more total area is covered by the surfactant by virtue of increased concentration, what remains after evaporation is largely contained in one formation, not evenly distributed over the coverage area. On hydrophobic substrates, the single island remaining post-evaporation covers approximately 10% of that covered by the hydrophilic substrate: 2.5 mm^2 at 30% RH and 3−5 mm^2 for 80% RH conditions, representing between 4 and 13% of the maximum area.

By manipulating the concentration of surfactant, the distribution and mean island size can be controlled. Given similar contact angle droplets on leaf surfaces, it is expected that similar deposition patterns also will form. This study provides a firm ground on what to expect for given combinations of humidity, concentration, and droplet/substrate contact angle as imaging methods are developed for visualizing surfactant residues on specific leaf surfaces.

LITERATURE CITED

(1) Picknett, R. G.; Bexon, R. The Evaporation of Sessile or Pendant Drops in Still Air. *J. Colloid Interface Sci.* **1977**, *61* (2), 336–350.

(2) Birdi, K. S.; Vu, D. T.; Winter, A. A study of the Evaporation Rates of Small Water Drops Placed on a Solid Surface. *J. Phys. Chem.* **1989**, *93*, 3702–3703.

(3) Erbil, H. Y.; McHale, G.; Rowan, S. M.; Newton, M. I. Analysis of Evaporating Droplets Using Ellipsoidal Cap Geometry. *J. Adhes. Sci. Technol.* **1999**, *13* (12), 1375–1391.

(4) Sikalo, S.; Wilhelm, H. D.; Roisman, I. V.; Jakirlic, S.; Tropea, C. Dynamic Contact Angle of Spreading Droplets: Experiments and Simulations. *Phys. Fluids* **2005**, *17*, 061203.

(5) Clay, M. A.; Miksis, M. J. Effects of Surfactant on Droplet Spreading. *Phys. Fluids* **2004**, *16* (8), 3070–3078.

(6) Deegan, R. D.; Bakajin, O.; Dupont, T. F.; Huber, G.; Nagel, S. R.; Witten, T. A. Capillary-Flow as The Cause of Ring Stains from Dried Liquid-Drops. *Nature* **1997**, *389* (6653), 827–829.

(7) Hu, H.; Larson, R. G. Evaporation of a Sessile Droplet on a Substrate. *J. Phys. Chem. B* **2002**, *106* (6), 1334–1344.

(8) Hu, H.; Larson, R. G. Analysis of the Effects of Marangoni Stresses on the Microflow in an Evaporating Sessile Droplet. *Langmuir* **2005**, *21* (9), 3972–3980.

(9) Chen, Y. S.; Lu, Y. L.; Yang, Y. M.; Maa, J. R. Surfactant Effects on the Motion of a Droplet in Thermocapillary Migration. *Int. J. Multiphase Flow* **1997**, *23* (2), 325–335.

(10) Edmonstone, B. D.; Matar, O. K. Simultaneous Thermal and Surfactant-Induced Marangoni Effects in Thin Liquid Films. *J. Colloid Interface Sci.* **2004**, *274* (1), 183–199.

(11) Sefiane, K. Effect of Nonionic Surfactant on Wetting Behavior of an Evaporating Drop under a Reduced Pressure Environment. *J. Colloid Interface Sci.* **2004**, *272* (2), 411.

(12) Mulqueen, M.; Datwani, S. S.; Stebe, K. J.; Blankschtein, D. Dynamic Surface Tensions of Aqueous Surfactant Mixtures: Experimental Investigation. *Langmuir* **2001**, *17* (24), 7494–7500.

(13) McCallion, O. N.; Taylor, K. M.; Thomas, M.; Taylor, A. J. The Influence of Surface-Tension on Aerosols Produced by Medical Nebulizers. *Int. J. Pharm.* **1996**, *129*, 1–2.

(14) Truskett, V.; Stebe, K. J. Influence of Surfactants on an Evaporating Drop: Fluorescence Images and Particle Deposition Patterns. *Langmuir* **2003**, *19* (20), 8271–8279.

(15) Nguyen, V. X.; Stebe, K. J. Patterning of Small Particles by a Surfactant-Enhanced Marangoni−Benard Instability. *Phys. Rev. Lett.* **2002**, *8816* (16), 4501.

(16) Hopwood, J. D.; Mann, S. Synthesis Of Barium-Sulfate Nanoparticles and Nanofilaments in Reverse Micelles and Microemulsions. *Chem. Mater.* **1997**, *9* (8), 1819–1828.

(17) Basu, S.; Luthra, J.; Nigam, K. D. P. The Effects of Surfactants on Adhesion, Spreading, and Retention of Herbicide Droplet on the Surface of the Leaves and Seeds. *J. Environ. Sci. Health, Part B* **2002**, *37* (4), 331–344.

(18) Zhu, H.; Reichard, D. L.; Fox, R. D.; Brazee, R. D.; Ozkan, H. E. Simulation of Drift of Discrete Sizes of Water Droplets from Field Sprayers. *Transactions of the ASAE* **1994**, *37* (5), 1401–1407.